INVESTIGATIONS ON LASER BEAM WELDING OF HIGH-MANGANESE AUSTENITIC AND AUSTENITIC-FERRITIC STAINLESS STEELS

V. QUIROZ, A. GUMENYUK and **M. RETHMEIER**
BAM Federal Institute for Materials Research and Testing, Berlin, Germany

4.4 kW Nd:YAG laser and 5 kW CO_2 laser were applied to welding 1.5 mm stainless steel sheets in CW mode. Manganese austenitic and lean duplex steels were selected as test materials and for comparison with standard austenitic and duplex steels. The influence of main laser welding parameters on process stability and resulting weld quality, as well as the effects of weld edge preparation on the weld appearance and quality levels, were investigated. The welded joints obtained were subjected to radiographic tests for detection of internal imperfections, tensile and potentiodynamic tests were performed to evaluate the mechanical and corrosion properties. The results provide an insight into the advantages and limitations of the laser beam welding process for joining high-manganese alloyed stainless steels. Conditions for the production of defect-free and corrosion-resistant welds having good mechanical properties could be determined.

Keywords: *laser welding, CO_2- and Nd:YAG laser, stainless austenitic and duplex steels, higher manganese content, process stability, shielding atmosphere, weld metal, microstructure, mechanical properties, corrosion resistance*

Instabilities in the nickel price as a consequence of the high demand for stainless steels and, for instance, current forecasts of supply shortages in feedstock [1] are driving the introduction of more cost effective alternatives. The partial substitution of less expensive manganese and small amounts of nitrogen for nickel in austenitic and duplex stainless steels has been reported to be a viable option [2–6]. The role of nitrogen is crucial, as it helps to stabilize the austenite phase and further results in increased strength and work hardening [7] without affecting the ductility properties of the material [8]. That is favourable for weight reduction and better energy absorption in crash [9].

Corrosion, microstructure and mechanical properties of various CrMnNi-steels have already been extensively investigated [3, 6, 10–13]. However, weldability is still an insufficiently explored aspect. In this respect, the laser welding method offers several advantages in comparison with other processes as high welding speed and low heat input, which reduces effectively component distortion and metallurgical damage. Laser weldability is closely related to some specific process characteristics. The keyhole and, consequently, process stability can, for example, intensively be affected by the laser type and parameters [14]. This directly influences the weld quality, as spatter, underfilling, humping and porosity may arise in dependence of the keyhole behaviour. Furthermore, the high resulting cooling rate can alter the weld metal phase balance, when welding duplex stainless steels, as the austenite formation, which is primarily controlled by the diffusion of nitrogen, is diminished [15].

In this study, laser welding experiments applying two different laser sources was carried out with the objective of analysing the influences of corresponding process specificities on weldability of the austenitic and austenitic-ferritic CrMnNi-steel, in comparison with standard CrNi-steel grades. The obtained weld quality was examined in terms of weld appearance, internal imperfections, microstructure, as well as resulting corrosion and mechanical properties.

Experimental. For the investigations, the austenitic CrMnNi 1.4376 and lean duplex 1.4162 steels were selected as test materials. The standard austenitic 1.4301 and duplex 1.4362 steels were chosen for comparison. Chemical composition of the materials investigated is given in Table 1. All sheets had thickness of 1.5 mm.

Table 1. Chemical composition of the investigated materials, wt.%

	C	Cr	Ni	Mn	Si	P	S	Cu	Nb	Mo	N
1.4376	0.03	18.03	5.09	6.55	0.42	0.023	0.005	0.23	0.01	0.10	0.15
1.4301	0.04	18.82	8.79	1.36	0.38	0.027	0.004	0.45	0.01	0.19	0.05
1.4162	0.04	22.42	1.83	3.84	0.34	0.028	0.004	0.43	0.01	0.11	0.14
1.4362	0.03	22.86	4.33	1.40	0.002	0.023	0.002	0.52	0.01	0.13	0.12
Fe — balance.											

Table 2. Laser characteristics

	CO_2 laser	Nd:YAG laser
Wavelength, μm	10.6	1.064
Laser beam delivery	Mirror	600 μm fibre
BPP, mm·mrad	17 (TEM_{20})	24
Focal distance, mm	200	200
Focus diameter, μm	~400	~600

Table 3. Laser welding parameters investigated

	Butt welding			Overlap welding		
	P_L, kW	v_w, m/min	F, mm	P_L, kW	v_w, m/min	F, mm
CO_2	2.4	3	0	2.4	2.5	0
	3.6	4		3.6	3.0	
	5.0	6		5.0	6.0; 7.0	
Nd:YAG	2.0	3	0	2.0	2.0	0; −3
				3.0	3.0	
				4.0	4.0; 5.0	

Welding was performed with 4.4 kW Nd:YAG and 5 kW CO_2 laser. Data on their characteristics are listed in Table 2.

Experiments were conducted in butt and overlap joint configurations. The effects of the weld edge preparation by using laser cutting or shear cut edges on weld quality were investigated for butt joints. Shielding gas for Nd:YAG laser welding was argon. For welding experiments with the CO_2 laser, a mixture of helium and argon (50/50) was necessary to suppress plasma. The shielding gas was applied coaxially. In addition, experiments were carried out with a trail gas nozzle. In case of the duplex steels, nitrogen was applied as shielding gas in order to examine its influence on the austenite reformation in weld metal. Pure argon was used as forming gas for butt welding. Other investigated welding variables were the shielding gas flow rate, focal point position F, laser power P_L and welding speed v_w (Table 3).

Radiographic non-destructive testing was used for evaluation of the weld internal imperfections. Cross sections of the welds were produced using conventional techniques to analyse the resulting microstructure. The obtained austenite fraction in the duplex steel weld metal was assessed by image analysis. The Vickers microhardness was determined at a load of 0.5 kg, and the weld tensile properties were determined for 4 transverse specimens.

Potentiodynamic experiments in salt solution (pH 4.5) were carried out at the room temperature to investigate pitting corrosion of all base materials, as well as of the produced butt and overlap joints. A standard hydrogen electrode (SHE) was used as reference one. The critical pitting (E_{cr}) and repassivation (E_{rep}) potentials were determined for pickled and non-pickled samples from dynamic cyclic anodic polarization curves. E_{cr} and E_{rep} were obtained from the points, where, respectively, the current density continuously exceeds 0.01 mA·cm^{-2}, and where the current density again goes near zero.

Results and discussion. *Process stability and weld quality*. Spatter formation proved to be related with several process variables. It was found, for example, that spatter was much more pronounced by using the Nd:YAG laser (Figure 1). This may be linked to the missing stabilizing effect of plasma, which is given in case of the CO_2 laser, at least in the keyhole depth.

High manganese content in the steel grade also had negative effect on the process stability. Vaporization of this volatile element enhanced melt expelling from the weld pool [16]. Another factor affecting the process stability was the focal point position (see Figure 1). By choosing the focus point in the negative range, spattering was considerably reduced. In addition, spattering was more severe in the overlap joints in comparison with butt ones. High shielding gas flow rates also supported spatter formation by causing instabilities on the weld pool behaviour. A stable spatter-free process could be achieved with flow rate up to about 20 l/min.

Oxidation of the weld surface and heat tint formation was influenced by the shielding gas type and supply. By CO_2 laser welding the use of a bypass led to a better weld surface quality. Complete oxidation prevention was successfully achieved for both laser welding processes with the additional trail gas nozzle.

The weld geometry was found to be strongly dependent on the joint edge quality. Shear cut joint preparations provided an irregular sheet edge geometry which resulted into gap sizes far exceeding the desired zero gap. Figure 2, *a* shows, for example, irregular weld shape with top bead depression and root concavity for this case. On the other hand, weld edge preparation by laser cutting led to a satisfactory weld geometry (Figure 2, *b*). A further advantage concerns the possibility to integrate laser welding and cutting, which may bring advantages in industrial processing.

Radiographic examinations detected no cracks for either CO_2- or Nd:YAG-welds. Pore formation was found to be dependent on the laser process, penetration mode, material and welding speed. Intense porosity only occurred at partial penetration in the overlap joints and was considerably more severe for Nd:YAG

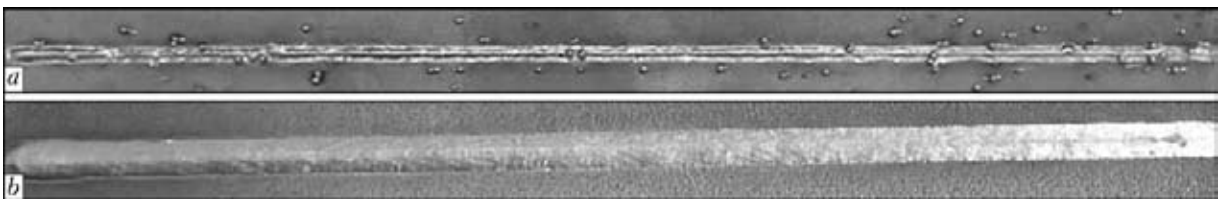

Figure 1. Spattering in the 150 mm weld zone in welding with Nd:YAG laser at v_w = 4 m/min, F = 0 (*a*) and −3 (*b*) mm

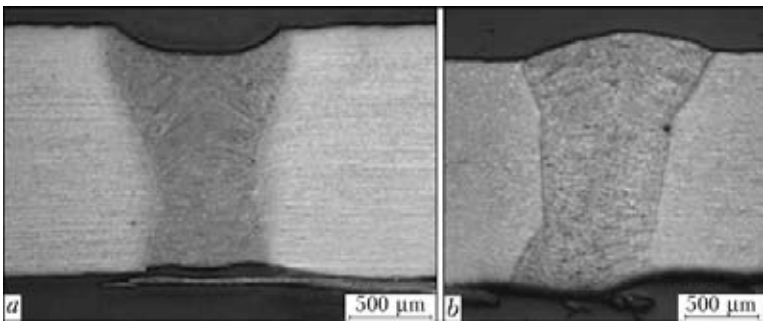

Figure 2. Butt weld with shear (*a*) and laser (*b*) cut edges

Table 4. Cr/Ni equivalents and solidification mode for all studied materials according to H&S and Hull diagrams

Material	H&S			Hull			Solidification
	Cr_{eq}	Ni_{eq}	Cr_{eq}/Ni_{eq}	Cr_{eq}	Ni_{eq}	Cr_{eq}/Ni_{eq}	
1.4376	18.82	10.14	1.86	18.35	9.40	1.95	FA
1.4162	23.10	6.32	3.66	22.72	6.00	3.79	F
1.4301	19.67	11.25	1.75	19.23	11.04	1.74	FA
1.4362	23.06	7.65	3.02	23.02	7.66	3.01	F

laser welding. It only arose at the lowest investigated welding speeds in the standard CrNi-steels (1.4301 and 1.4362). This may be explained in the keyhole behaviour. At low welding speeds, unstable melt flow leads to swelling of the keyhole, causing bubbles to generate from the keyhole tip in an unstable molten pool. In contrast, at high welding speeds the better keyhole stability can be reached [14].

Microstructure. Both studied austenitic steels underwent a primary ferrite solidification. This was determined from Cr/Ni equivalents (Table 4) and confirmed in microstructural examinations. The Hammer and Svenson (H&S) and Hull diagrams provided a tolerable correlation between the composition and the solidification mode, taking into account the special austenitizing effect of manganese.

Rapid cooling resulting from laser welding led to dendritic structure with retained delta-ferrite (Figure 3). The cooling rate also influenced the amount of primary ferrite. At high rates, transformation of reduced amount of delta-ferrite to austenite was occurred.

Duplex stainless steels owe their specific properties to the balanced two-phase microstructure consisting of ferrite and austenite of approximately equal proportions. The weld metal solidified in a ferritic mode, as predicted by H&S Cr/Ni equivalents.

By application of 100 % N_2, a maximal austenite content of about 20 % was obtained. In comparison with the specimens welded only in argon or argon/helium atmosphere, the austenite content values considerably increased (Figure 4).

No significant differences were found between the nitrogen absorption in Nd:YAG- or CO_2-laser welding under the conditions investigated.

Figure 4 also reveals that the lean duplex steel 1.4162 has a lower capacity for austenite reformation, which can be explained in the poorer austenitizing properties of manganese, compared to nickel.

In general, the effect of nitrogen on austenite formation is limited, because its absorption is hindered by the small weld pool surface and the higher partial pressure of metal vapour in the keyhole [17]. In the micrographs of both duplex steels 1.4362 and 1.4162 (see Figure 4) welded in 100 % N_2 atmosphere mainly allotriomorphic grain boundary austenite, but also small amounts of intergranular austenite precipitates can be observed.

Figure 5 shows the Vickers microhardness measurements in the centre of the weld cross sections. These

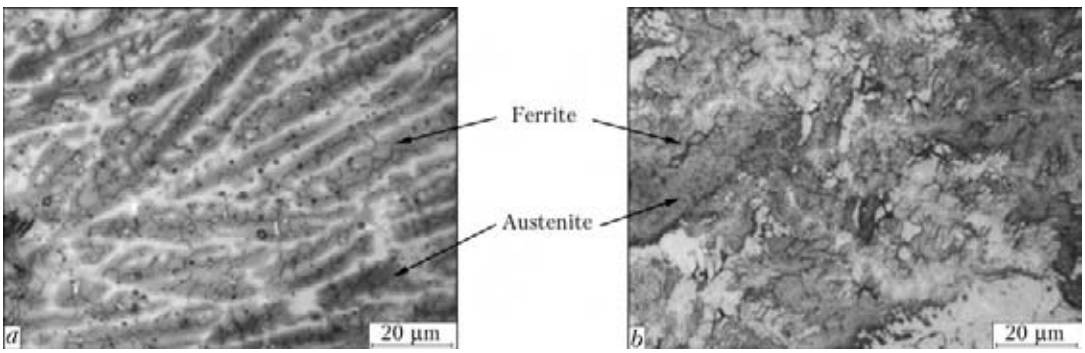

Figure 3. Steel 1.4301 (*a*) and 1.4376 (*b*) weld microstructure

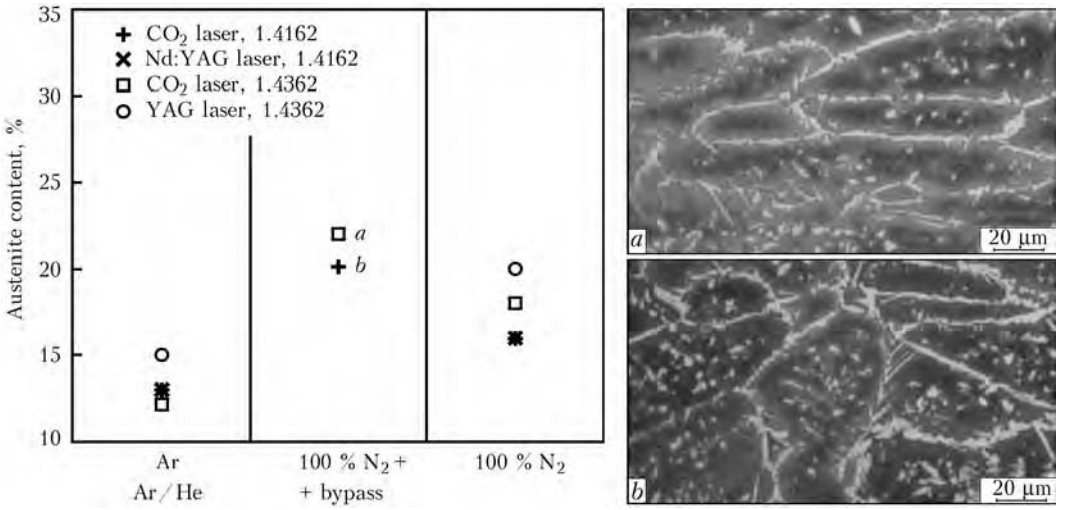

Figure 4. Austenite content in duplex steel welds obtained in CO_2- and Nd:YAG laser welding with and without nitrogen addition, and their microstructure (for explanation see the text)

reveal an increase of hardness in the weld metal for both duplex steels welded with 100 % N_2. The higher ferrite content and effect of nitrogen led to an increment of the hardness in this area. In the HAZ and in the bulk material similar lower values are obtained.

Regarding the austenitic steels, only a slight increase can be observed from the base material to HAZ and weld. Hardness of austenitic stainless steel 1.4376 is higher in comparison with standard CrNi-steel which results from the higher nitrogen content.

Mechanical properties. The mechanical properties of the investigated materials are mainly characterized by the corresponding microstructure. Austenitic stainless steels owe high work hardening properties and can achieve elongations of 50 %. The austenitic high-manganese alloyed steel possesses not only a high strength due to the higher nitrogen content, but also a good formability. Duplex steels have better properties than the austenitic ones due to the combination of strength and ductility provided by the ferrite and austenite phases, respectively. However, the enhanced amount of ferrite in the weld metal, in consequence of the high cooling rates, is expected to influence the mechanical properties.

The results of tensile tests of 4 welded samples per investigated material transversally to the welding direction show that the strength of the welded joints is close to that of the base material (Table 5).

Table 5. Tensile strength of base metal and welded samples, MPa

Steel	1.4376	1.4301	1.4162*	1.4362*
Base metal	750	650	750	770
Sample 1	740	665	750	760
Sample 2	755	655	750	765
Sample 3	700**	655	750	550**
Sample 4	750	655	750	760*

*Welded in 100 % N_2 atmosphere. **Fractured along the fusion line.

Failure occurred predominantly in the base material. Only single sample of steel 1.4376 and 1.4362 was fractured along the fusion line, which led to a reduction of the measured tensile strength.

Corrosion properties. The results of potentiodynamic tests revealed the austenitic stainless steel 1.4301 to exhibit the higher E_{cr} and E_{rep} potentials in comparison with the manganese-alloyed steel 1.4376, indicating a superior pitting resistance (Figure 6). According to the obtained E_{cr} values, the austenitic steel 1.4301 is approximately equivalent to the lean duplex steel 1.4162, and CrNi-duplex steel 1.4362 had the highest E_{cr} values.

Since the chromium content for both austenitic and also for both duplex stainless steels is similar (see Table 1), it appears that nickel has decisive influence on the corrosion properties of the materials. In study [11] it could be demonstrated that nickel is enriched in the surface during active dissolution, which does not apply to manganese. This is supposed to support the passive film formation, as in this way the dissolution rate decreases. The influence of manganese on corrosion resistance is also related to the increased amount of inclusions, e.g. manganese and chromium oxides that act as preferential sites of pitting [6]. The pitting corrosion behaviour of butt as

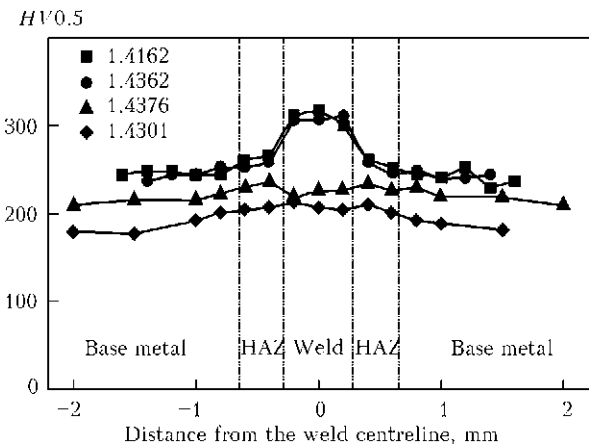

Figure 5. Hardness measurements in the middle of weld metal on all materials investigated

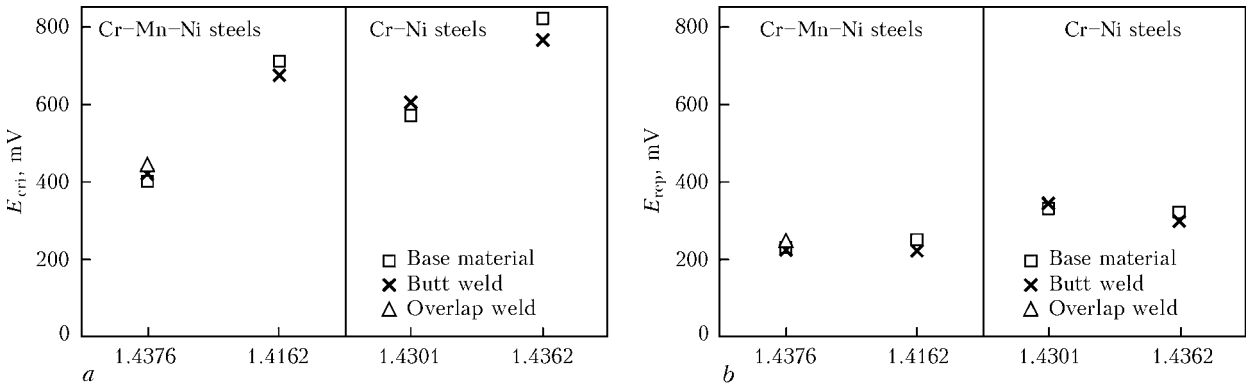

Figure 6. Critical pitting E_{cr} (*a*) and repassivation E_{rep} (*b*) potentials obtained from anodic current density/potential curves for all investigated previously pickled materials

well as overlap welds and base materials is comparable in all cases (see Figure 6). This indicates that a good weld quality can be obtained under the investigated conditions.

CONCLUSIONS

CO_2- and Nd:YAG laser welding of austenitic and austenitic-ferritic manganese-alloyed stainless steels was proven to be suitable for the production of high quality butt and overlap welded joints. Welds on all the investigated materials showed strength, hardness and corrosion performance that is consistent with or close to that of the base metal. Though following aspects need to be considered:

- manganese-alloyed steels are, in comparison with standard CrNi-steels, more prone to cause process instabilities that led to spatter formation;
- porosity tends to arise by incomplete penetration in the overlap joint and is highly influenced by the welding speed. Though, it was possible to avoid weld imperfections by adequate parameter settings;
- temper colours on the weld surface can be prevented by using a trail gas nozzle behind the weld;
- regarding the weld edge preparation, laser cutting is more effective than shear cutting as it allows the gap size reduction and weld homogeneity;
- the use of nitrogen as shielding gas during laser welding of duplex steels improves austenite reformation. Maximal austenite fraction in the weld of 20 % could be obtained. Although the austenite proportion is not so large, a good weld quality can be achieved;
- concerning the corrosion properties, the lean duplex steel 1.4162 was found to be comparable with the conventional steel 1.4301. The austenitic manganese-alloyed steel 1.4376 exhibited the lowest corrosion resistance, and standard duplex steel 1.4362 — the highest.

Acknowledgements. *The authors would like to thank the Federation of Industrial Research Associations (AiF Arbeitsgemeinschaft industrieller Forschungsvereinigungen) and the German Federal Ministry for Trade, Industry and Technology (BMWi Bundesministerium fur Wirtschaft und Technologie) for making this research possible by funding it in the Project 16208 N «Laser Beam Welding of Austenitic and Austenitic-Ferritic CrMnNi-Steels». Karin Schlechter, Marco Lammers, Karen Stelling and Marina Marten greatly contributed to the experimental part of the presented results.*

1. Hunt, B. (2010) *Nickel in perspective*. Wood Mackenzie.
2. Charles, J. (2007) The new 200-series: An alternative answer to Ni surcharge? Risks and opportunities? *La Revue de Metallurgie*, June, 308–317.
3. Kim, K., Kim, Y, Lee, Y. et al. (2004) Application study of an automotive structural part with Ni-alloyed high strength austenitic stainless steel: Paper 2001-01-0884. In: *Proc. of SAE World Congress*, 2004.
4. Klueh, R.L., Maziasz, P.J., Lee, E.H. (1988) Manganese as an austenite stabilizer in Fe–Cr–Mn–C-steels. *Materials Sci. and Eng. A*, 102(**1**), 115–124.
5. Singhal, L.K. (2006) Stainless steels recent developments and outlook: Demand, capacity and product development. In: *Joint India/OECD/IISI Workshop*, Vol. 15, 21.
6. Toor, I., Hyun, P.J., Kwon, H.S. (2008) Development of high Mn–N duplex stainless steel for automobile structural components. *Corrosion Sci.*, 50(**2**), 404–410.
7. Zuev, L.B., Dubovik, N.A., Pak, V.E. (1997) Nature of hardening of high-nitrogen steels based on iron-chromium-manganese austenite. *Stal*, 27(**10**), 71–75.
8. Myslowicki, S. (2007) *Das Auscheidungs- und Korrosionsverhalten eines stickstofflegierten, austenitischen Chrom-Nickel-Stahls mit abgesenkten Nickelgehalt*. Aachen: Shaker.
9. Ratte, E., Leonhardt, S., Bleck, W. et al. (2006) Energy absorption behaviour of austenitic and duplex stainless steels in a crash box geometry. *Steel Res. Int.*, 77(**9/10**), 692–697.
10. Honeycombe, J., Gooch, T.G. (1972) Effect of manganese on cracking and corrosion behavior of fully austenitic stainless steel weld metals. *Metal Construction and British Welding J.*, 4(**12**), 456–460.
11. Falkenberg, F., Johansson, E., Larsson, J. (2007) Properties of various low-nickel stainless steels in comparison to AISI 304. In: *Proc. of Stainless Steel World Conf. & Expo 2007* (Maastricht, the Netherlands), 355–371.
12. Tzaneva, B.R., Fachikov, L.B., Raicheff, R.G. (2006) Pitting corrosion of Cr–Mn–N steel in sulphuric acid media. *J. Appl. Electrochemistry*, 36(**3**), 347–353.
13. Zardiackas, L.D., Williamson, S., Roach, M. et al. (2003) Comparison of anodic polarization and galvanic corrosion of a low-nickel stainless steel to 316LS and 22Cr–13Ni–5Mn stainless steels. In: *Stainless steels for medical and surgical applications*, 107–118.
14. Katayama, S. (2009) Fundamentals of fiber laser welding. In: *Proc. of Int. Colloquium on High Power Laser Welding* (Berlin).
15. Amigo, V., Bonach, E.V., Teruel, L. et al. (2006) Mechanical properties of duplex stainless steel laser joints. *Welding Int.*, 20(**5**), 361–366.
16. Brooks, J.A. (1975) Weldability of high N, high Mn austenitic stainless steel. *Welding Res. Suppl.*, 189–195.
17. Dong, W., Kokawa, H., Sato, Y. et al. (2003) Nitrogen absorption by iron and stainless steels during CO_2 laser welding. *Metall. and Mater. Transact. B*, Febr., 75–82.